Supporting Information

Non-covalent Cross-linking to Boost the Stability and Permeability of Graphene-oxide-based Membranes

Jin Ran*[1], Chengquan Chu[1], Ting Pan[1], Liang Ding[2], Peng Cui*[1], Cen-Feng Fu[3], Chuan-Ling Zhang[1], Tongwen Xu*[2]

1. School of Chemistry and Chemical Engineering, School of Material Science and Engineering, Hefei University of Technology, Hefei, Anhui 230009, P.R. China;

2. Lab of Functional Membranes, School of Chemistry and Material Science, University of Science and Technology of China, Hefei 230026, P.R. China;

3. Department of Chemical Physics, School of Chemistry and Material Science, University of Science and Technology of China, Hefei 230026, P.R. China

* Corresponding author. E-mail: ranjin@mail.ustc.edu.cn; twxu@ustc.edu.cn; cuipeng@hfut.edu.cn

Experimental details

1. **Materials.** Graphene oxide (GO) powders were purchased from XFNANO Materials Tech Co. Ltd. (Nanjing, China). Brominated poly(2,6-dimethyl-1,4-phenylene oxide) (Br-PPO) and sulfonated poly(2,6-dimethyl-1,4-phenylene oxide) (S-PPO) were kindly provided by Tianwei Membrane Co., Ltd. (Shandong, China). The commercial Br-PPO and S-PPO were purified by dissolving them into NMP, precipitating into methanol, and dried at 40 ^{o}C. The -CH_2Br proportion in Br-PPO in relative to the benzene rings number was 50% confirmed by ^{1}H NMR. Polyvinylidene fluoride (PVDF) microfiltration membranes were purchased from Jinteng experimental equipment Co. Ltd (China). 1,2-Dimethylimidazole was purchased from Alfa Aesar Chemical Co. Ltd. (China). N-methyl-2-pyrrolidolone (NMP, AR grade), potassium chloride (KCl, AR grade), sodium chloride (NaCl, AR grade), calcium chloride ($CaCl_2$, AR grade), magnesium chloride ($MgCl_2$, AR grade), methyl blue (MB, AR grade), rhodamine B (RB, AR grade), methylene blue (MLB, AR grade), evans blue (EB, AR grade), basic fuchsin (BF, AR grade) and sucrose (AR grade) were purchased from Shanghai-Sinopham Chemical Reagent Co. Ltd.(China). Deionized (DI) water was used throughout the experiments.

2. **Synthesis of imidazolium functionalized Br-PPO (Im-PPO)**.[1] 1 g of Br-PPO was dissolved into 10 mL NMP to obtain homogeneous solutions. Then, 0.3 g of 1,2-dimethylimidazole was added to guarantee the complete conversion of -CH_2Br and the resulting mixtures were stirred at 40 ^{o}C overnight. Afterwards, the solution was poured into excess water to gain solid Im-PPO. The redundant 1,2-dimethylimidazole was removed by washing the solids with large amounts of water for several times. The final polymers were dried under vacuum at 60 ^{o}C overnight.

3. **Synthesis of GO and GO composite membranes.** The marketed GO powers were dispersed in water (0.1 mg/mL) and subsequently sonicated for 1 h to prepare GO nanosheets solutions. The purified S-PPO were dissolved using N-methyl-2-pyrrolidolone (NMP) as solvents (10 mg/mL). Similarly, 10 mg/mL of Im-PPO

solutions (NMP used as solvents) were prepared for the subsequent membrane preparation.

Certain amounts of GO solutions and S-PPO solutions (or Im-PPO solutions) were mixed to get required ratios of ionic polymers in relative to GO (0.1, 0.5 and 1.0). The mixture were violently stirred for 1 h, and sonicated for 1 h to make the mixture to be uniform enough. Then, the blending solutions were further diluted (0.0025 mg/mL) for the composite membranes preparation and the GO solutions were also diluted (0.0025 mg/mL) for the pure GO membranes preparation.

GO, S-PPO intercalated GO (anions doping GO, dominated as A-GO), and Im-PPO intercalated GO (cations doping GO, dominated as C-GO) membranes were fabricated by vacuum filtration of corresponding suspensions through PVDF microfiltration membranes with a pore size of 0.22 μm (47 mm in diameter). These membranes were dried under vacuum at 40 ^{o}C for 24 h prior to use. For the preparation of wet membranes, the resulting membranes were immediately immersed into water to maintain them in solvated states.

4. Characterizations. ^{1}H NMR spectra of polymers were recorded on Bruker 510 instrument operating at 400 MHz. Fourier transform infrared (FT-IR) spectra of polymers and membranes were recorded on LX10-8813 (USA). Scanning electronic microscopy (SEM) images were taken out by using a SU8020 scanning electron microscope (Hitachi, Japan) with an accelerating voltage of 10 kV. X-ray diffraction (XRD) was performed on a X'Pert PRO MPD X-ray diffractometer with Cu Kα radiation (λ = 0.15418 nm, Palmer naco, Netherland). Atomic force microscope (AFM) images were recorded on an SPM 9600 microscope (Shimadzu, Japan). Raman spectra were obtained by the use of a LabRAM HR Evolution (HORIBA Jobin Yvon, France) Raman microscope with a 532 nm laser. X-ray photoelectron spectroscopy (XPS) spectra were collected by using an ESCALAB 250XI photoelectron spectrometer (ThermoFisher Scientific, USA). UV-vis spectra were carried out on a UV-2550 spectrophotometer (Shimadzu, Japan). Zeta potential tests were conducted on a Nano-ZS90 zeta potential analyzer (Malvern, England) by using standard condition.

4. **Water permeability and dye rejection of performances**. Water permeability experiments were performed using a home-made nanofiltration equipment working under a cross-flowing mode with a pressure difference of 1.0 bar or a dead-end filtration device used for high pressure filtration tests (**Figure S12**). The effective filtration area is 7.07 cm^2 (one circular domain with a diameter of 3 cm). All the as-testing membranes were firstly filtrated with pure water until constant fluxes were attainable. The concentrations of dyes in water range from 10 to 50 μmol/L, depending on the absorbance of the observed dyes. The resulting concentrations of feed, permeate, and retentate solutions were determined by the UV-vis spectrophotometer. All the data of permeances and rejection rates were gained from the average value of the measurements of three individual membranes. The permeance J (L m^{-2} h^{-1} bar^{-1}) and rejection R (%) were calculated according to the equations (1) and (2), respectively:

$$J = \frac{V}{A\Delta t \Delta P} \qquad (1)$$

$$R = \left(1 - \frac{C_p}{C_f}\right) \times 100\% \qquad (2)$$

Where V (L) refers to the volume of permeated water, A (m^2) is the effective filtration area, Δt (h) is the filtration time, ΔP (bar) is the transmembrane pressure, and C_p and C_f are the concentration of the permeate and feed solutions, respectively.

5. **Salts rejection and water permeation in the forward osmosis (FO) processes**. Salts rejection experiments were conducted using a bespoke H-beaker setup. GO and GO composite membranes supported by the PVDF substrates were sealed by a piece of copper tape containing a hole with a diameter of 8 mm (an effective area of 0.5 cm^2) in its center. The two compartments in this device were filled with equal volumes (100 mL) of 0.2 mol/L salts (NaCl, KCl, $CaCl_2$, or $MgCl_2$) and water. Both of the feed and permeate sides undergo continuing stirring to minimize the concentration polarization through the testing. The ionic conductivity of permeate side was recorded every interval 1 h, and the measurements last 3 h. The measured ionic conductivity variations of

permeate solutions were converted to corresponding salts concentrations according to the molar conductivity calculations.[2] Salts rejection R_s (%) was calculated on the basis of the equation (3):

$$R_s = \left(1 - \frac{C_{GO}}{C_{PVDF}}\right) \times 100\% \qquad (3)$$

Where C_{GO} and C_{PVDF} are the increasing ions concentration in the permeate sides when the GO-based membranes are present and absent, respectively.

For the water permeation tests in FO, equal volumes (100 mL) of DI water and 3 M sucrose draw solution were filled into the feed and permeate sides, respectively. 3 M sucrose will lead to 75 bar osmotic pressure gradient between two sides of the as-tested membranes, which provides extra forces to draw water from the feed to permeate sides. After 48 h permeation, the height changes of the sucrose compartment were recorded to determine the penetrative water volumes. All the data of rejection rates and water fluxes were gained from the average value of the measurements of three individual membranes. Then water fluxes F (L m^{-2} h^{-1}) were calculated on the basis of the equation (4):

$$F = \frac{\Delta V}{A \Delta t} \qquad (4)$$

Where ΔV (L) is the increasing volumes of the permeate side, A (m^2) is the effective area of permeation, and Δt (h) is the FO operating time.

6. Computation details.

The quantum mechanical calculations were carried out by the Gaussian 09 revision D.01 suite program.[3] The density functional theory (DFT) calculations were performed with the B3LYP hybrid functional. The split-valence 6-311++G(d,p) basis set was employed. The models used for graphene oxide (GO), imidazolium, and sulfonic acid are shown in the following **Figure S1**.

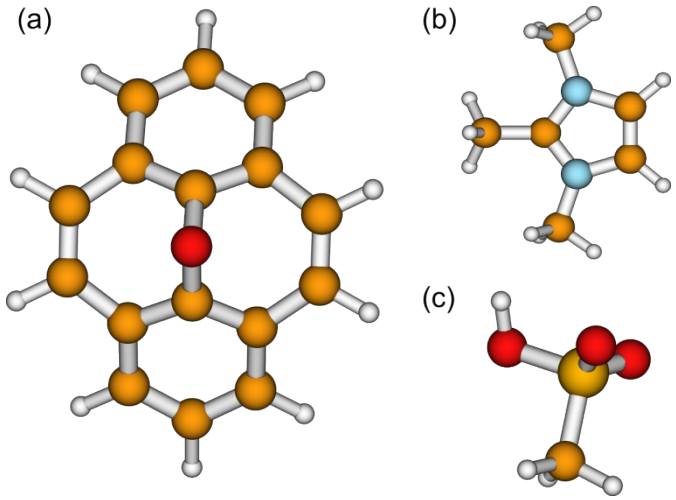

Figure S1. Models used for (a) GO, (b) imidazolium, and (c) sulfonic acid.

Firstly, the structures of isolated GO, imidazolium, and sulfonic acid were optimized. Then, the structures of GO-imidazolium and GO-sulfonic acid composites were optimized. The binding energies of these two composites were calculated by

$$\Delta E(GO\text{-}X) = E(GO\text{-}X) - E(GO) - E(X)$$

where X represents imidazolium or sulfonic acid. The corrections for the basis-set superposition error (BSSE) were included for the calculations of binding energies.

For GO-sulfonic acid composite, the O···H−O hydrogen band between the epoxy group of GO and the hydroxyl group of sulfonic acid was observed, and the calculated binding energy is -31.0 kJ/mol. For GO-imidazolium composite, the Mulliken charge analysis indicates that there are 0.151 electrons transferred from imidazolium to GO, and the calculated binding energy is -43.6 kJ/mol. These results reveal that the interaction between GO and imidazolium is much stronger than that between GO and sulfonic acid.

Figures

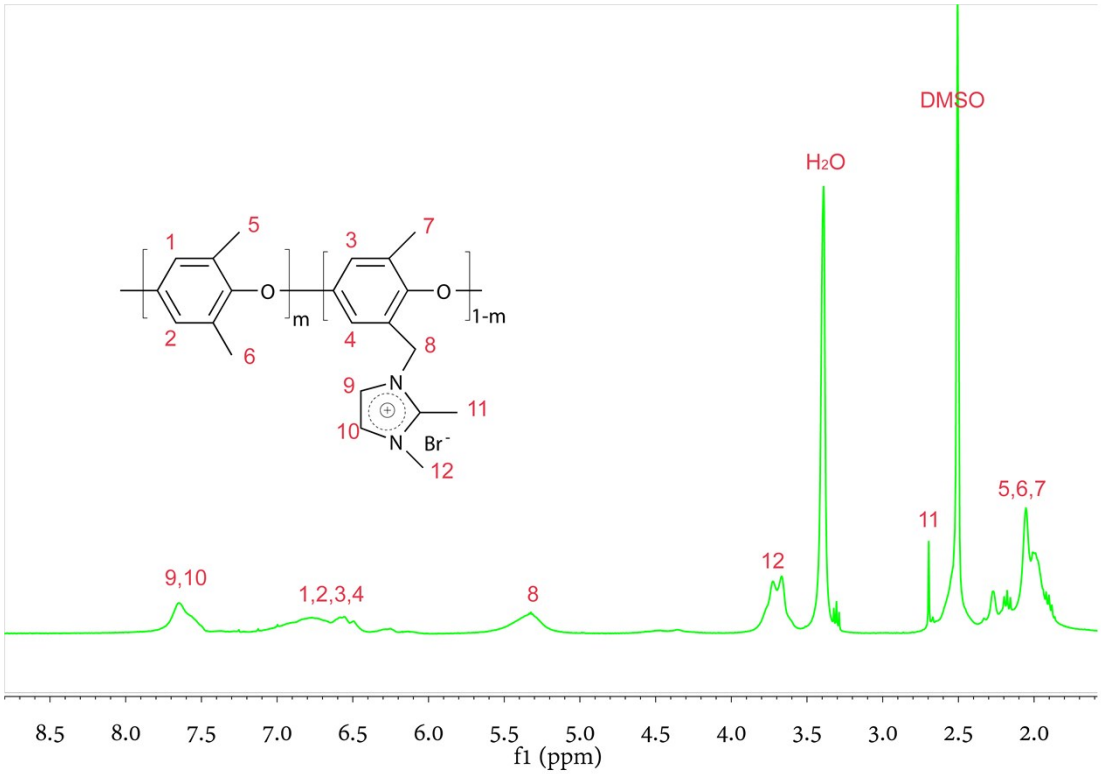

Figure S2. The ^{1}H NMR spectrum of Im-PPO.

Im-PPO was prepared by reacting BPPO with 1,2-dimethylimidazole. As shown in **Figure S2**, the peaks at 6.15-7.10 ppm are assignable to the aromatic protons (H1, H2, H3, H4), and the multiple peaks at 1.81-2.37 ppm arise from the methyl protons (H5, H6, H7). All these peaks belong to the PPO polymer backbone. The introduction of imidazolium (Im) cations can be manifested by the additional peak at 7.65 ppm, which corresponds to the methylene protons (H9, H10) on the Im ring. Moreover, the peaks at 2.70 ppm and 3.70 ppm due to the methyl protons (H11, H12) on the Im ring further indicate the success of Im functionalization.

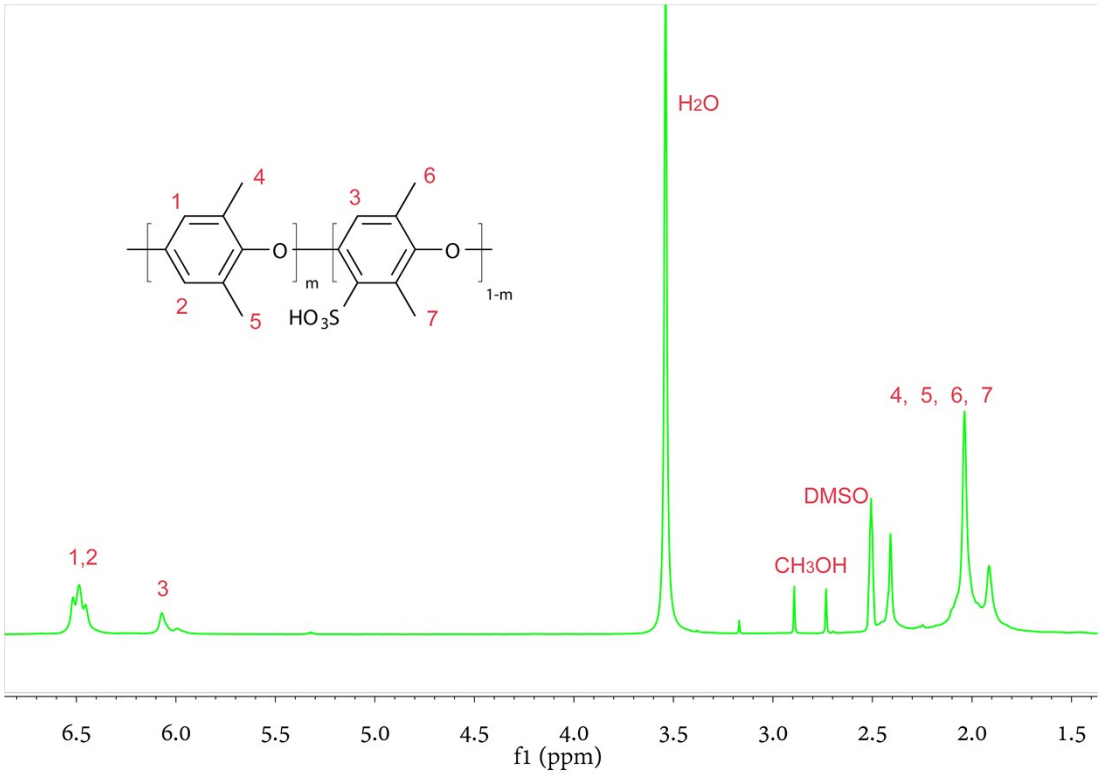

Figure S3. The ^{1}H NMR spectrum of S-PPO.

The chemical structure of S-PPO was identified by ^{1}H NMR. As shown in Figure S3, the peaks at 6.08 ppm and 6.48 ppm correspond to the protons (H1, H2, H3) on the aromatic rings functionalized by sulfonic acid groups and the pristine aromatic rings, respectively. The methyl protons (H4, H5, H6, H7) chemical shifts linking onto the benzene units lie in the range of 1.80-2.45 ppm. Due to the inevitable hydrogen exchange between sulfonic acid moieties and residue water in solvents, the proton signal of the sulfonic acid cannot be detected.

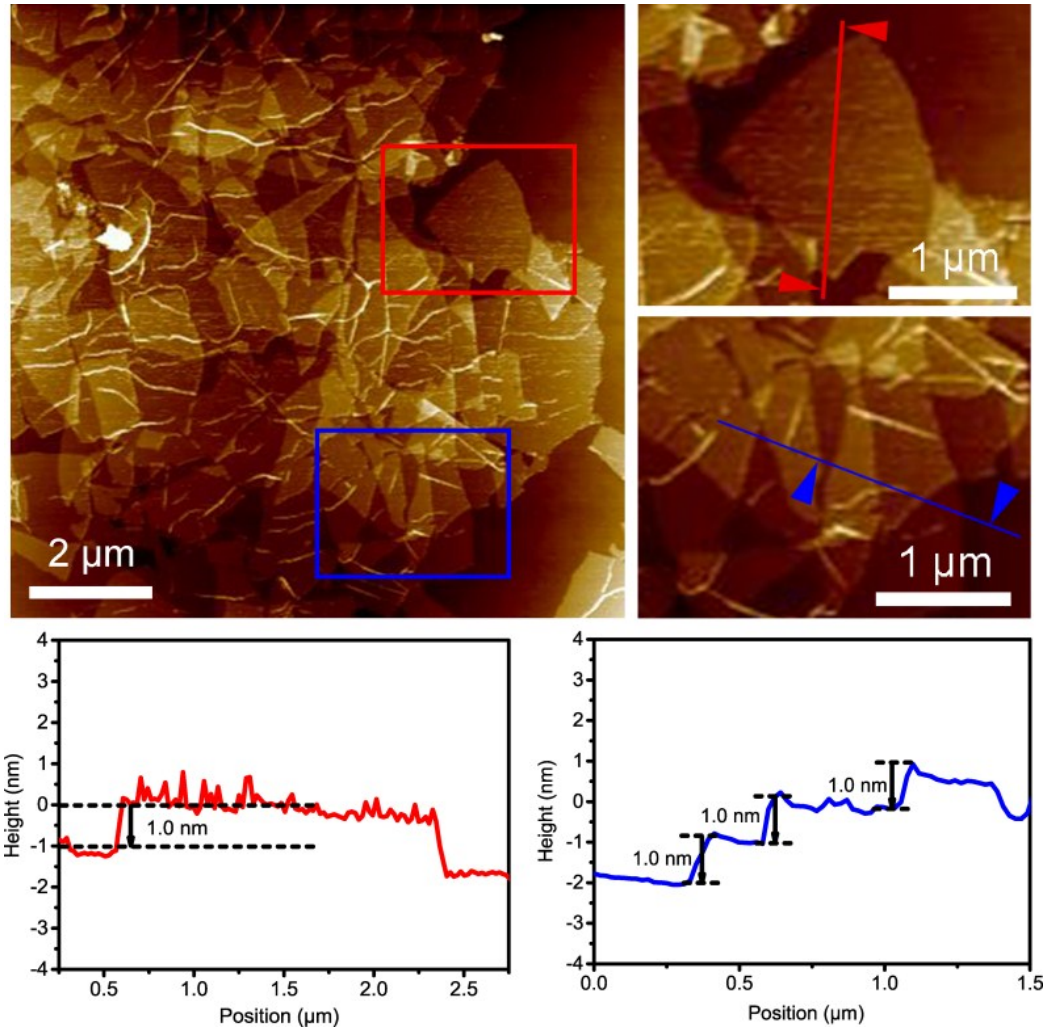

Figure S4. The AFM images and height profiles of GO nanosheets.

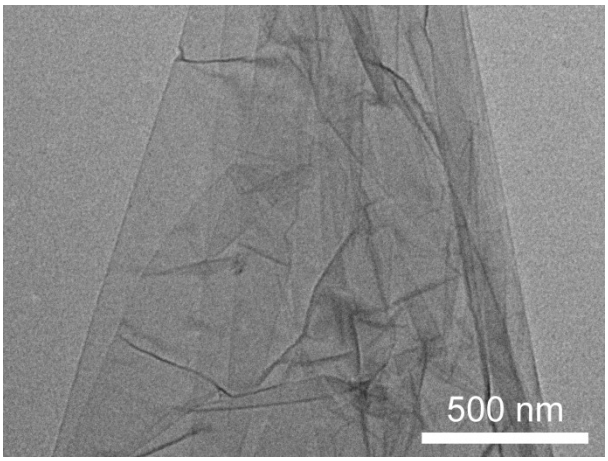

Figure S5. The TEM image of GO nanosheets.

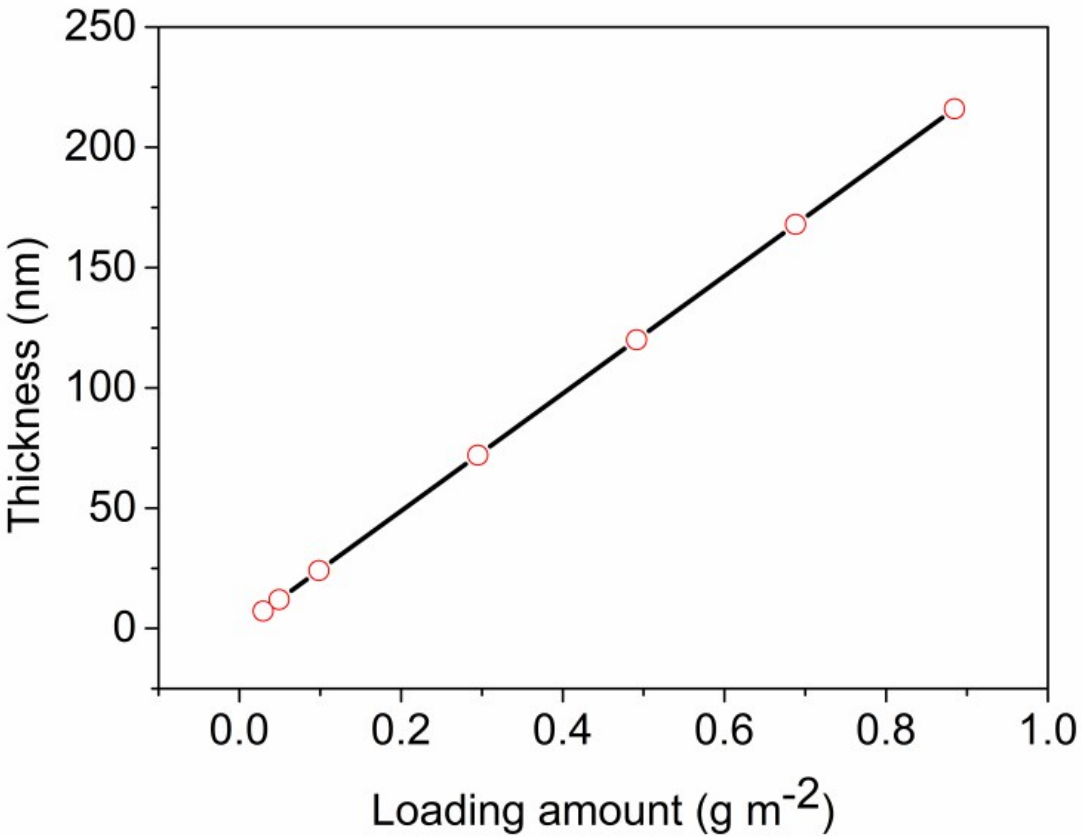

Figure S6. The GO membrane thickness variations as a function of GO loading amounts (the thicknesses are determined by the SEM observations).

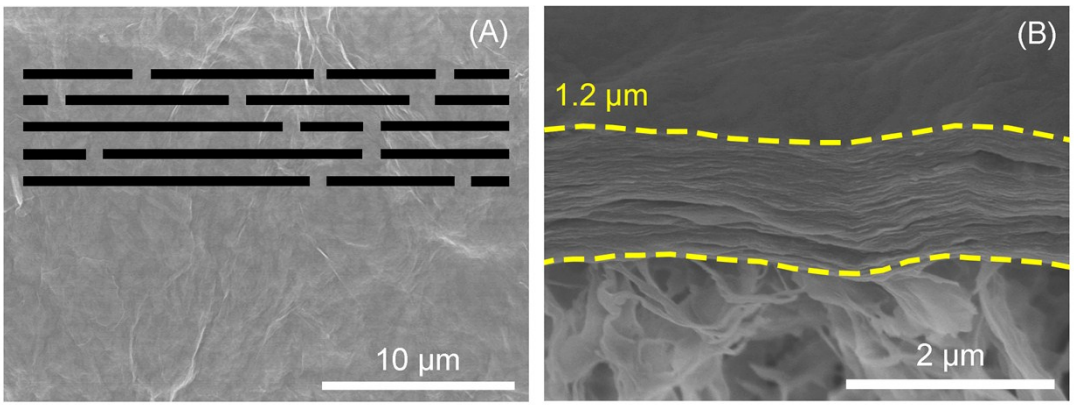

Figure S7. (A) The SEM image of the surface of the GO membrane. (B) The SEM cross-section image of the GO membrane.

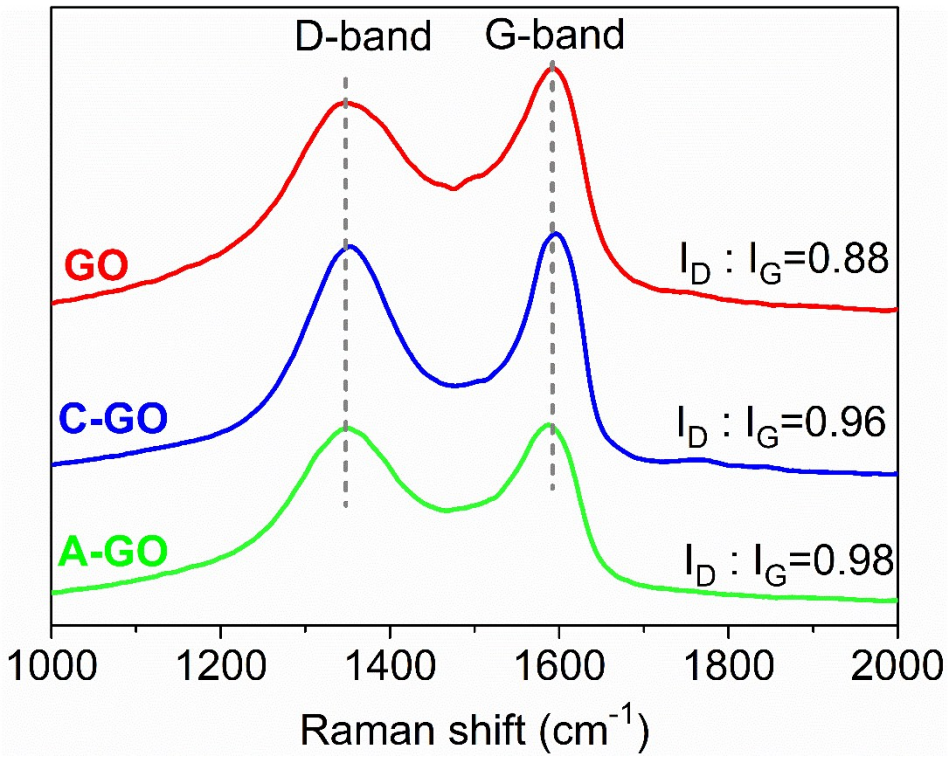

Figure S8. The Raman spectra of GO, C-GO and A-GO wave numbers from 1000-2000 cm^{-1}.

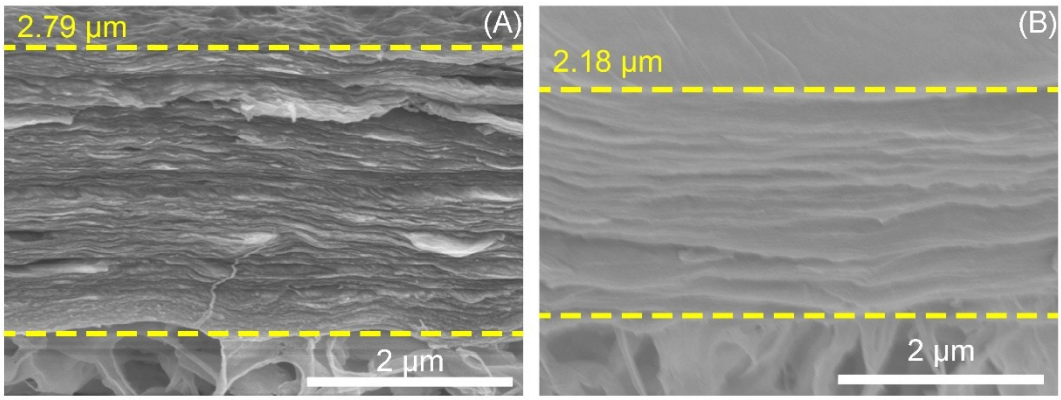

Figure S9. The SEM cross-sectional images of (A) C-GO and (B) A-GO membranes with a weight ratio of GO and polymers of 1 : 1.

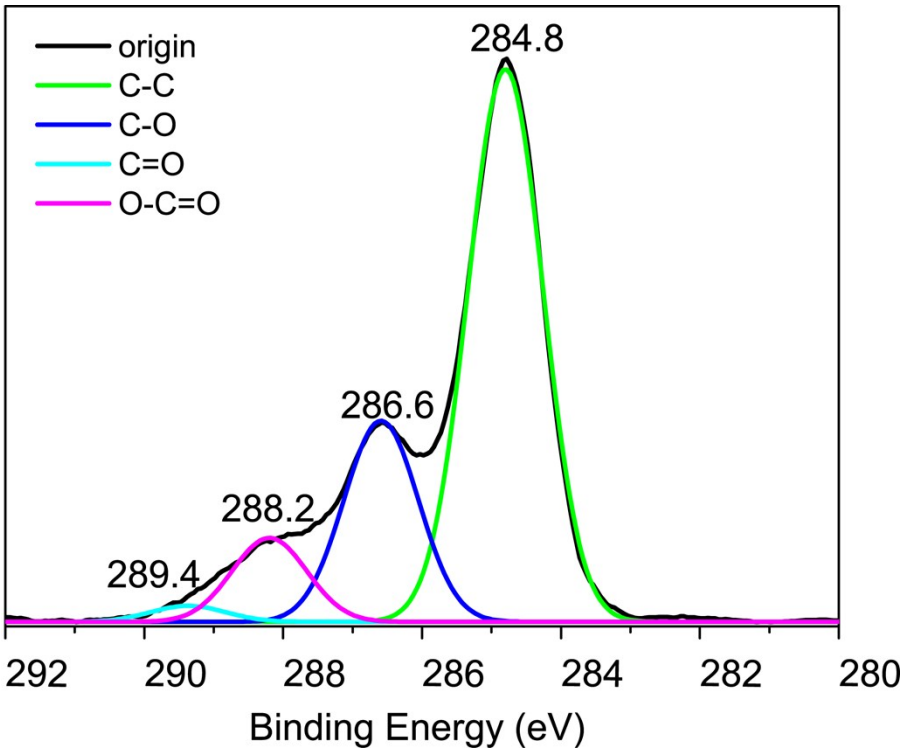

Figure S10. The C1s XPS spectra of GO.

In the C1s spectrum of GO, it can be seen that four kinds of C atoms (C-C, C-O, C=O, and C(O)O) exist in the GO sheets. The C-O contents account for 23.8% of the total C1s peak area, while the contents of C=O and C(O)O are 9.8% and 1.8%, respectively. This result indicates that the C/O atom ratio in GO is approximately 3/1.

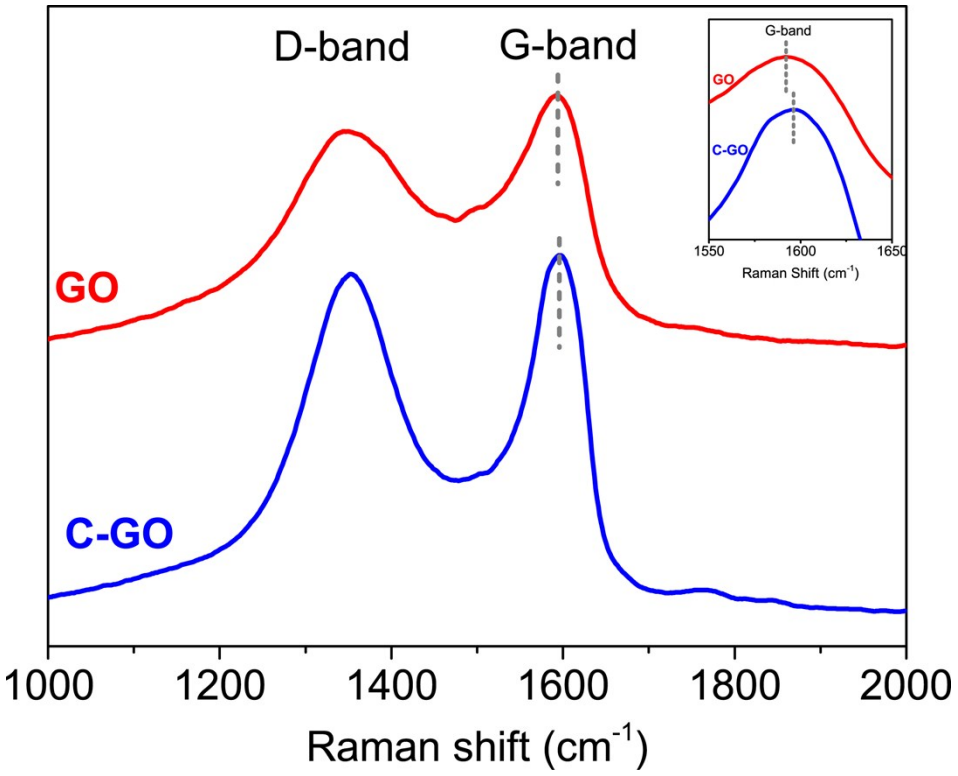

Figure S11. The Raman spectra of GO and C-GO wave numbers from 1000-2000 cm^{-1}, and wave numbers from 1550-1650 cm^{-1} (inset).

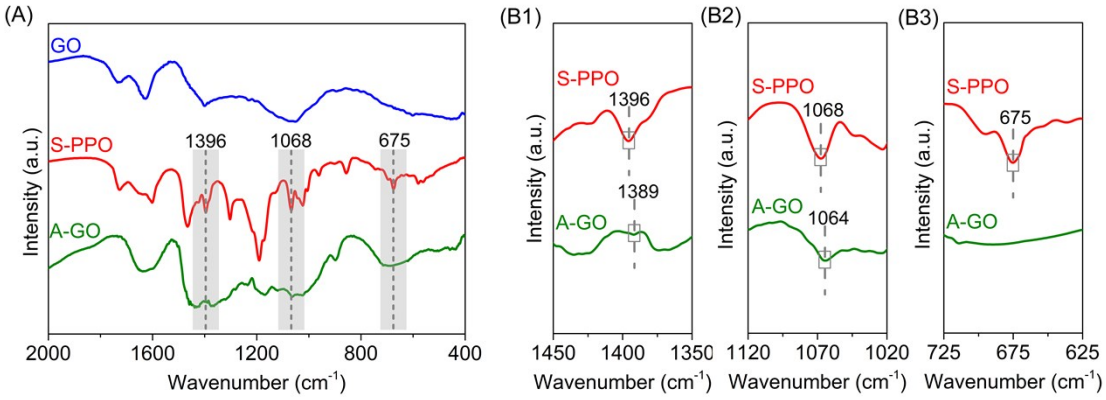

Figure S12. The FT-IR spectra of GO, S-PPO, and A-GO (A) wave numbers from 400-2000 cm^{-1}, (B1) wave numbers from 1350-1450 cm^{-1}, (B2) wave numbers from 1020-1120 cm^{-1}, (B3) wave numbers from 625-725 cm^{-1}.

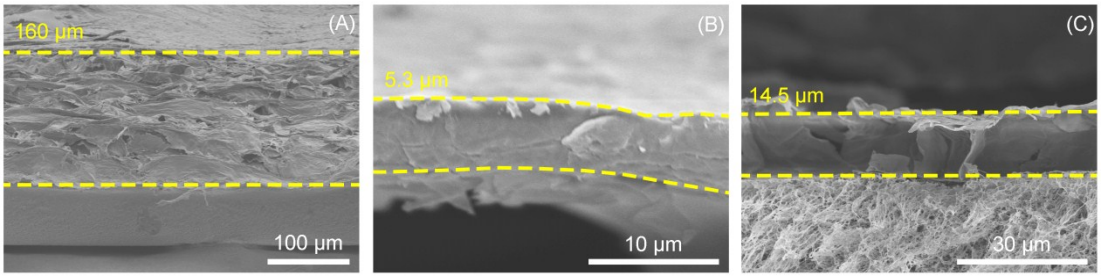

Figure S13. The SEM cross-section images of the freeze-dried solvated (A) GO, (B) C-GO and (C) A-GO membranes.

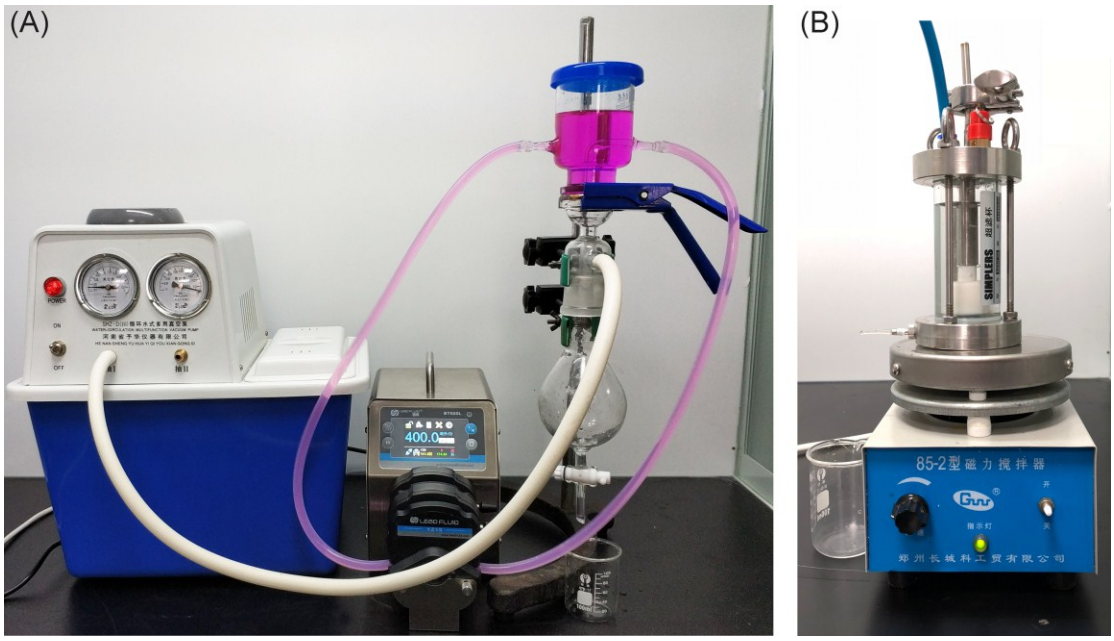

Figure S14. (A) The digital photo of the home-made cross flow filtration device. (B) The digital photo of the dead-end filtration device.

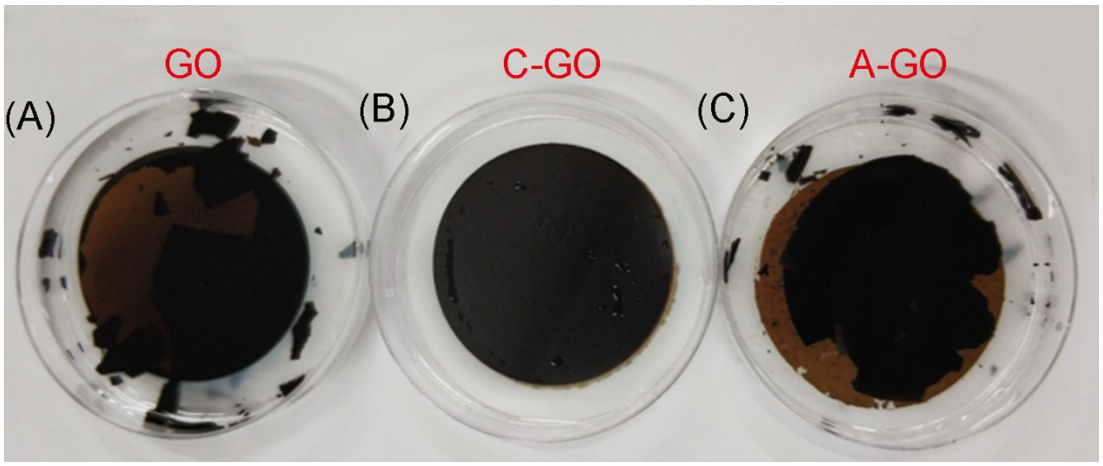

Figure S15. Photographs of (A) GO, (B) C-GO, and (C) A-GO membranes after 60 mins under cross flows of 400

mL min^{-1} at 1 bar.

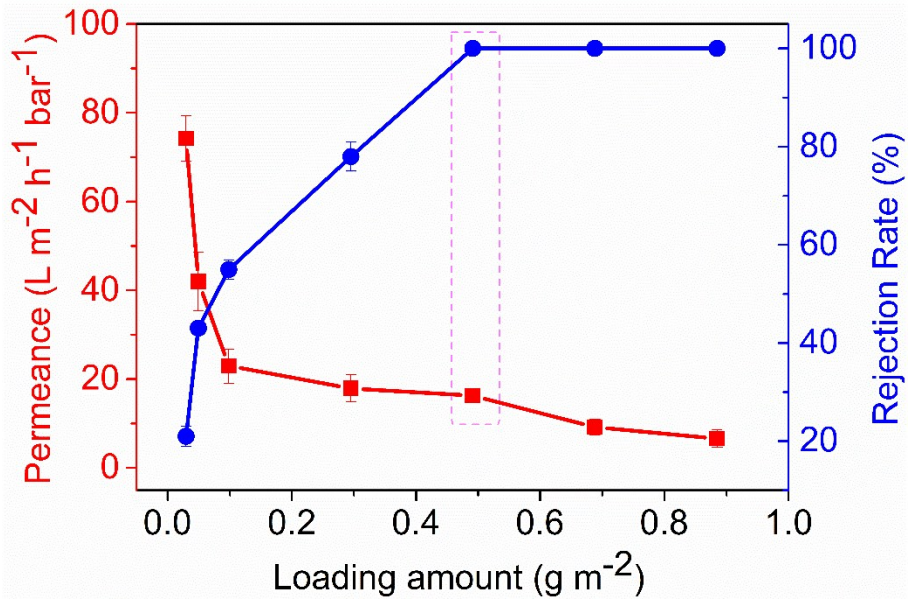

Figure S16. Dependence of separation performance of GO membranes on membrane thicknesses. The filtration solutions are MB dyes effluents.

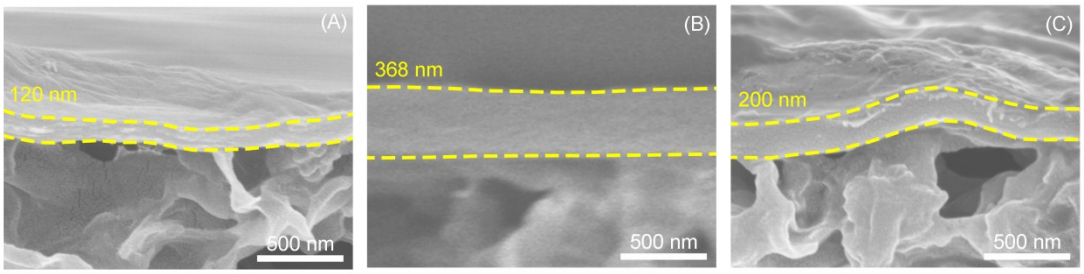

Figure S17. The SEM cross-section images of (A) GO, (B) C-GO, and (C) A-GO membranes (the GO loading amount is 0.5 g m^{-2}).

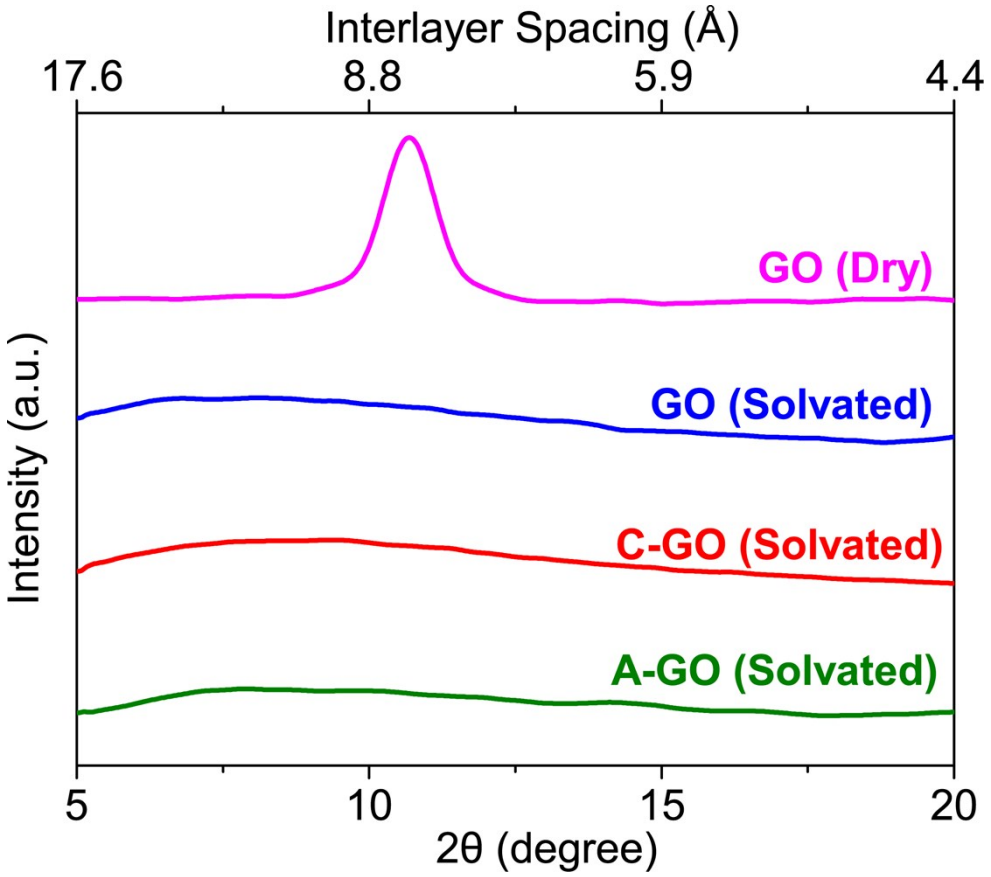

Figure S18. The XRD patterns of dry GO as well as solvated GO, C-GO and A-GO membranes in pure aqueous.

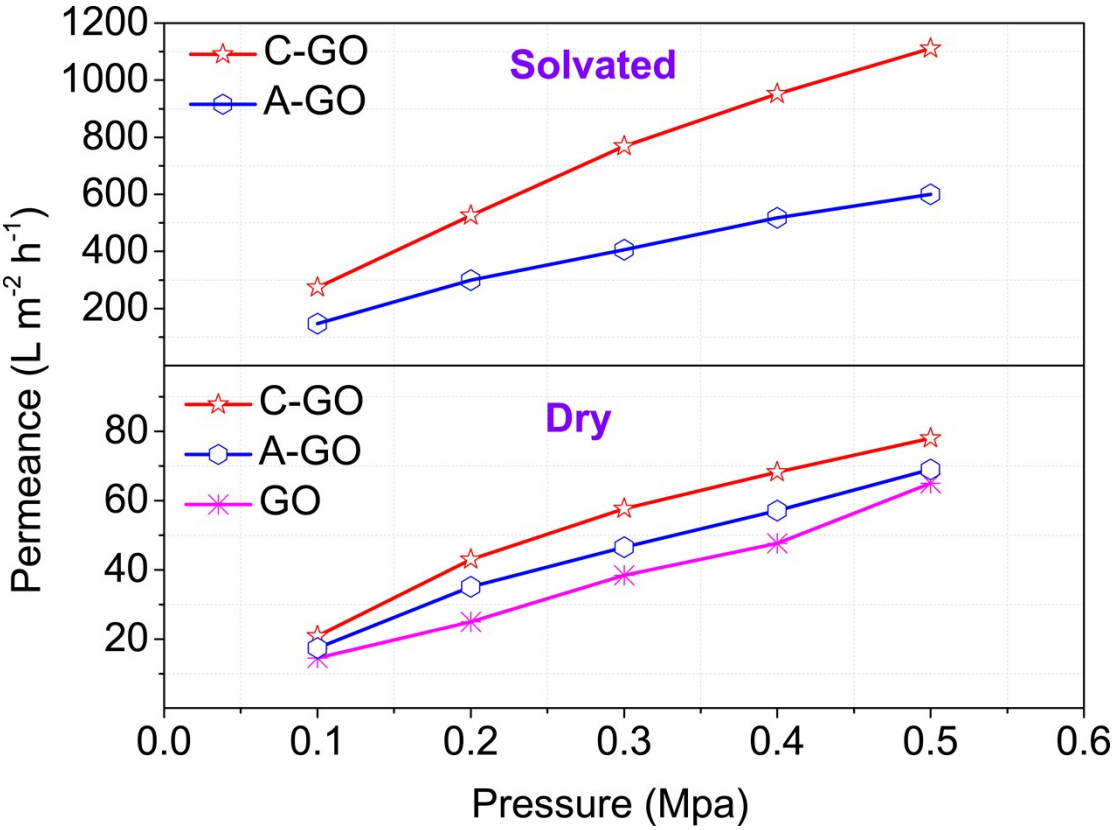

Figure S19. The plots of water permeance of dry GO, C-GO and A-GO membranes (down) as well as solvated C-GO, and A-GO membranes (up) as a function of pressure.

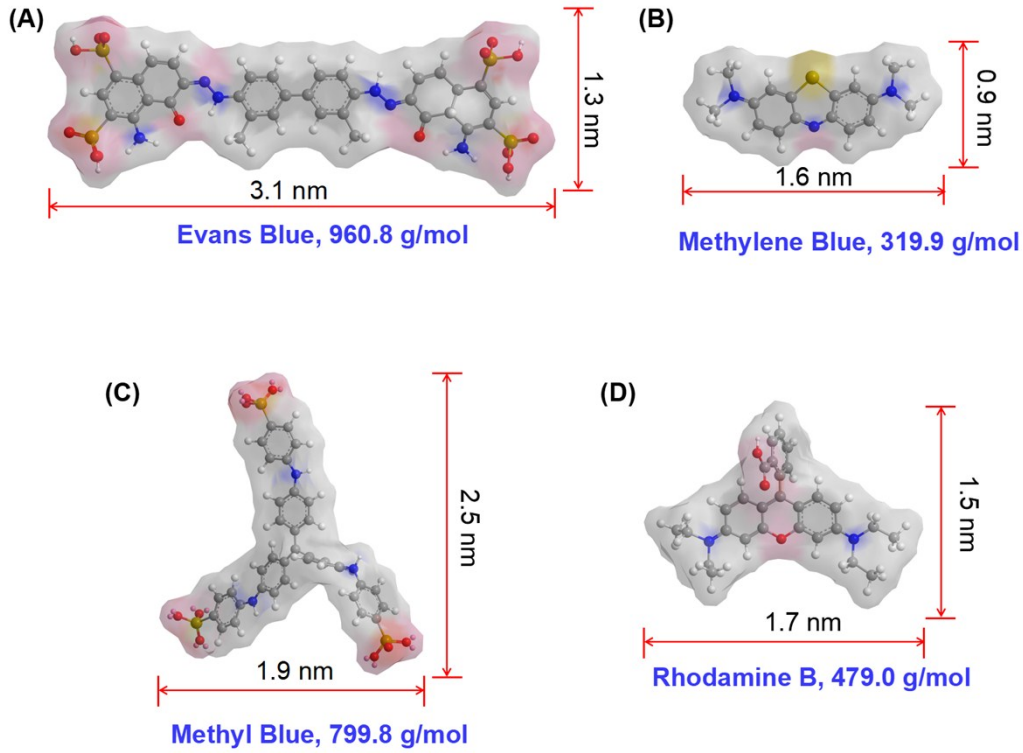

Figure S20. The chemical structures and sizes of the dyes used for the molecular separation experiments.

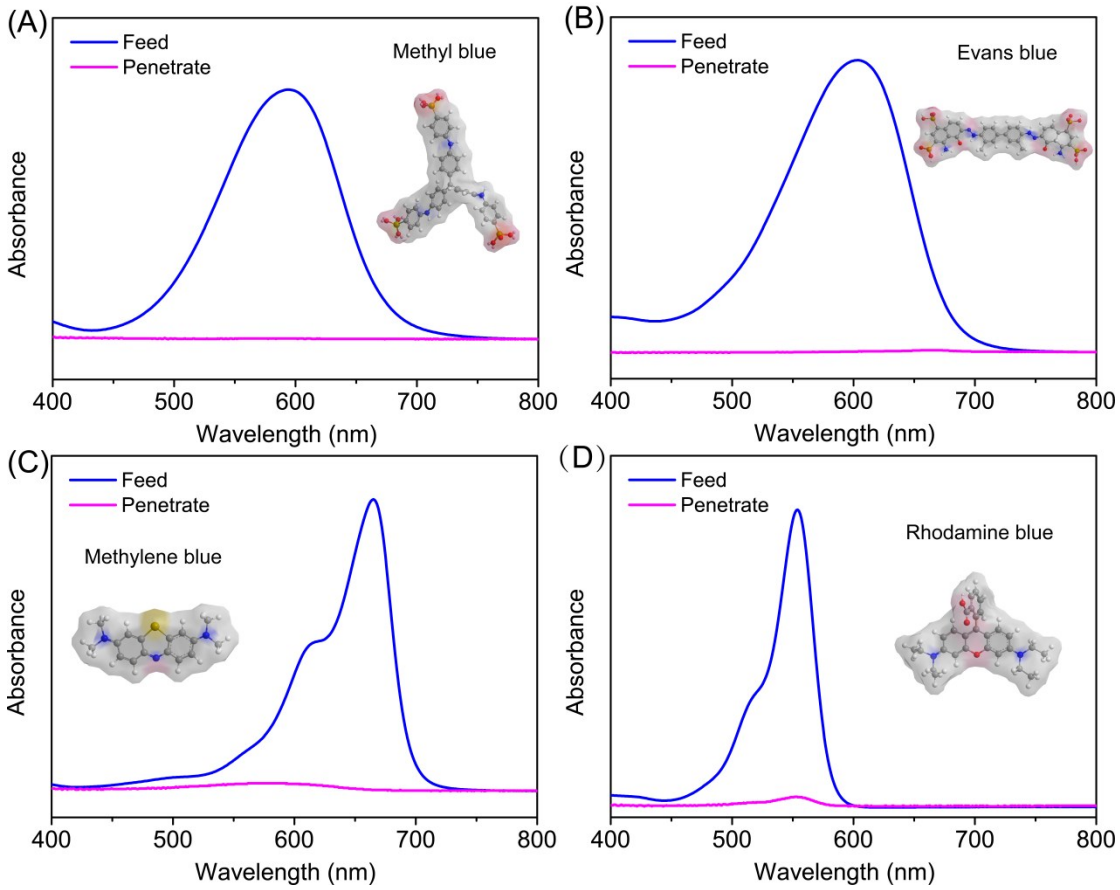

Figure S21. UV-vis absorption spectra of the feed, and the permeate of (A) MB, (B) EB, (C) MLB and (D) RB solution after filtration by the GO membrane.

Table S1. The separation performances of dry GO, C-GO and A-GO membranes as well as solvated C-GO and A-GO membranes for dyes with varied sizes and charges. MB and EB are negatively charged, and MLB and RB are positively charged. The unit of permeance is L m^{-2} h^{-1} bar^{-1}. The data shown here obtained by the composite membranes with a weight ratio of GO and polymers of 1 : 0.5.

Membrane	Water	MB (2.5 × 1.9 nm^2)		EB (3.1 × 1.3 nm^2)		MLB (1.6 × 0.9 nm^2)		RB (1.7 × 1.5 nm^2)	
	Perm.	Perm.[a)]	Rej.[b)]	Perm.	Rej.	Perm.	Rej.	Perm.	Rej.
GO (D)	15±1	16±2	100	12±4	100	16±5	100	13±5	84±4
C-GO ($D^{c)}$)	24±4	14±6	81±3	19±3	90±5	12±1	93±1	17±6	88±6
C-GO ($S^{d)}$)	389±16	284±23	100	276±9	99±1	281±5	99±1	281±5	96±3
A-GO (D)	17±4	23±2	92±5	17±4	92±5	17±8	95±2	19±4	88±4
A-GO (S)	135±14	127±8	100	116±8	100	103±11	100	130±3	93±1

a : Perm.: Permeance; b : Rej.: Rejection; c : D: Dry; d : S: Solvated.

Table S2. Benchmarking of GO-based membranes for organic dyes nanofiltration.

Membranes	Thickness	Dyes	Rejection (%)	Permeance (L m^{-2} h^{-1} bar^{-1})	Reference

GO/PNIPAM	1.1 μm	RB	68.2	16.53	[4]
		Cyt. c	99.8	7.98	
brGO	22 nm	MB	99.2	21.81	[5]
NSC-GO	1.85-2.17 μm	EB	87±3	279±20	[6]
44-GO	35.6 nm	EB	92.9	4.8±1.9	[7]
HEPI/S-rGO	18 nm	MB	98.6	85.4	[8]
		BF	97.5	86.5	
		EB	85.2	100	
rGO+CNT	1.23 μm	MB	98±2	52.7	[9]
]CCG	250 nm	DY	67	40	[10]
GO	150±15 nm	MB	95±5	71±5	[11]
GO/FLG	26-33 nm	RB	8	-	[12]
		AB9	96	-	
LGO	-	EB	89.59	66.9	[13]

GO/PNIPAM poly(N-isopropylacrylamide) covalent-grafted GO；brGO base-refluxing reduced GO; NSC-GO nanostrand-channeled graphene oxide; 44-GO GO mass loading 44 mg m-2; HEPI/S-rGO hyperbranched poly(ethylene imine)/solvent solvated reduced graphene oxide; CNTs carbon nanotubes; CCG chemically converted graphene; GO/FLG GO and few-layered graphene membrane; LGO lamellar graphene oxide; RB Rhodamine B; Cyt. c Cytochrome c; MB Methyl Blue; EB Evans Blue; BF Brilliant Yellow; DY Direct Yellow; AB9 Acid Blue 9.

Table S3. The water permeance and separation performances of dry GO and C-GO membranes for dyes with varied sizes and charges.

Dye molecule	GO		C-GO (0.1[a])		C-GO (0.5[a])		C-GO (1.0[a])	
	Permeance ($L\ m^{-2}\ h^{-1}\ bar^{-1}$)	Rejection (%)	Permeance ($L\ m^{-2}\ h^{-1}\ bar^{-1}$)	Rejection (%)	Permeance ($L\ m^{-2}\ h^{-1}\ bar^{-1}$)	Rejection (%)	Permeance ($L\ m^{-2}\ h^{-1}\ bar^{-1}$)	Rejection (%)
H_2O	15±1	-	21±2	-	24±4	-	19±1	-
MB	16±2	100	14±4	82±4	14±6	81±3	11±1	82±2
EB	12±4	100	18±3	95±3	19±3	90±5	17±1	85±1
MLB	16±5	100	14±1	99±1	12±1	93±1	22±4	95
RB	13±5	84±4	14±1	85±5	17±6	88±6	23±4	83±6

a : the bracket values are the weight ratios of GO and intercalation polymers.

Table S4. The water permeance and separation performances of dry GO and A-GO membranes for dyes with varied sizes and charges.

Dye molecule	GO		A-GO (0.1[a])		A-GO (0.5[a])		A-GO (1.0[a])	
	Permeance ($L\ m^{-2}\ h^{-1}\ bar^{-1}$)	Rejection (%)	Permeance ($L\ m^{-2}\ h^{-1}\ bar^{-1}$)	Rejection (%)	Permeance ($L\ m^{-2}\ h^{-1}\ bar^{-1}$)	Rejection (%)	Permeance ($L\ m^{-2}\ h^{-1}\ bar^{-1}$)	Rejection (%)
H_2O	15±1		15±3		17±4		15±2	
MB	16±2	100	16±3	98±2	23±2	92±5	20±3	96±3
EB	12±4	100	16±3	88±9	17±4	92±5	13±3	96±3
MLB	16±5	100	17±4	98±1	17±8	95±2	18±2	98±1
RB	13±5	84±4	15±5	86±4	19±4	88±4	12±2	89±3

a : the bracket values are the weight ratios of GO and intercalation polymers.

Table S5. The water permeance and separation performances of dry GO and solvated C-GO membranes for dyes with varied sizes and charges.

Dye molecule	GO		C-GO (0.1[a])		C-GO (0.5[a])		C-GO (1.0[a])	
	Permeance (L m^{-2} h^{-1} bar^{-1})	Rejection (%)	Permeance (L m^{-2} h^{-1} bar^{-1})	Rejection (%)	Permeance (L m^{-2} h^{-1} bar^{-1})	Rejection (%)	Permeance (L m^{-2} h^{-1} bar^{-1})	Rejection (%)
H_2O	15±1		374±34		389±16		259±16	
MB	16±2	100	263	100	284±23	100	163±17	100
EB	12±4	100	211±6	96±1	276±9	99±1	196±8	97
MLB	16±5	100	230	95±4	281±5	99±1	185±3	97
RB	13±5	84±4	211±6	84±7	281±5	96±3	178	90±5

a : the bracket values are the weight ratios of GO and intercalation polymers.

Table S6. The water permeance and separation performances of dry GO and solvated A-GO membranes for dyes with varied sizes and charges.

Dye molecule	GO		A-GO (0.1[a])		A-GO (0.5[a])		A-GO (1.0[a])	
	Permeance (L m^{-2} h^{-1} bar^{-1})	Rejection (%)	Permeance (L m^{-2} h^{-1} bar^{-1})	Rejection (%)	Permeance (L m^{-2} h^{-1} bar^{-1})	Rejection (%)	Permeance (L m^{-2} h^{-1} bar^{-1})	Rejection (%)
H_2O	15±1		131±6		135±14		153±9	
MB	16±2	100	130±3	100	127±8	100	133±5	100
EB	12±4	100	133±3	100	116±8	100	131±1	100
MLB	16±5	100	115±6	100	103±11	100	127±2	100
RB	13±5	84±4	141±3	96±1	130±3	93±1	165±8	94±1

a : the bracket values are the weight ratios of GO and intercalation polymers.

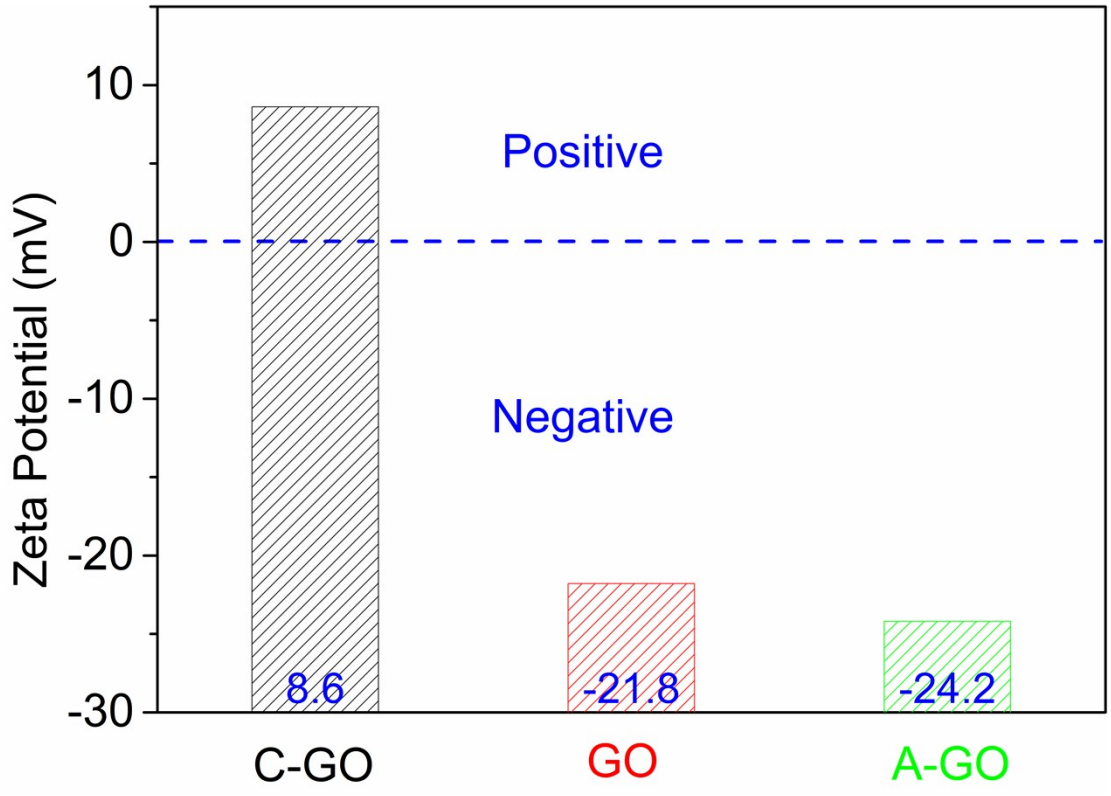

Figure S22. The zeta potentials of C-GO, GO, and A-GO.

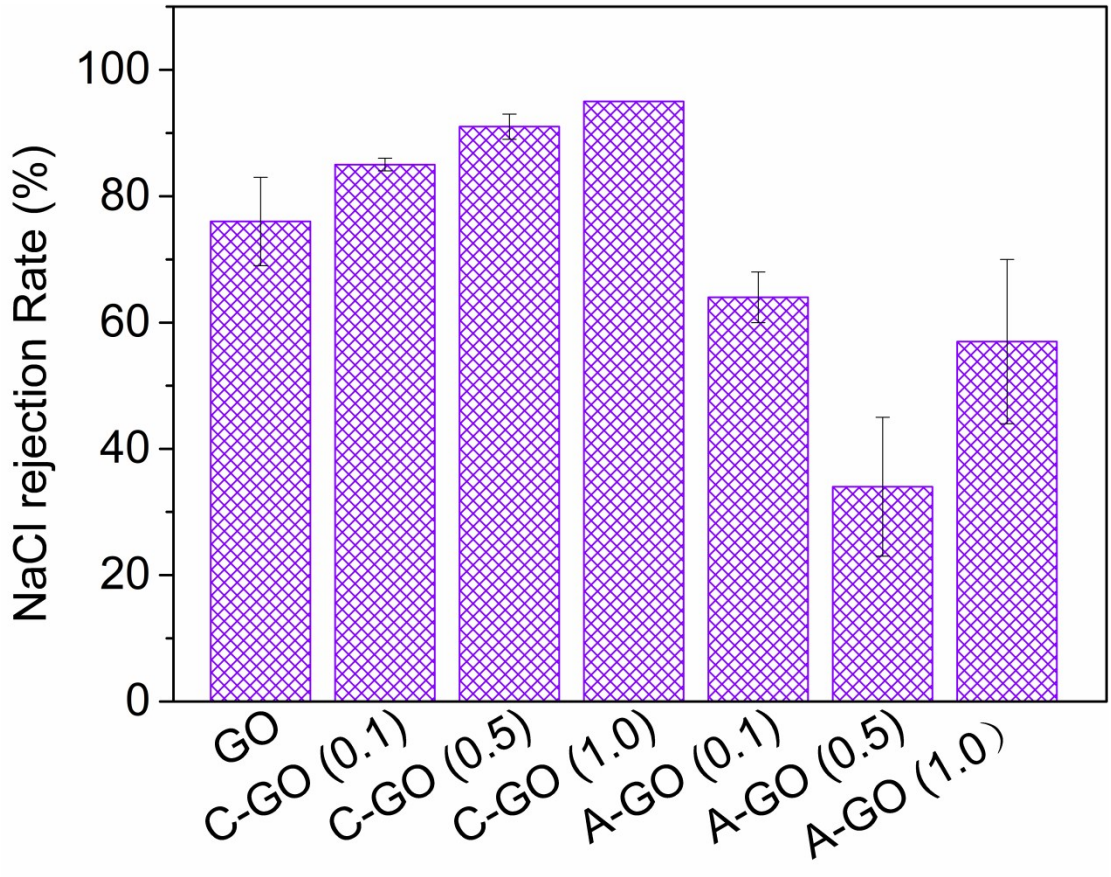

Figure S23. The NaCl rejection properties of GO, C-GO, and A-GO membranes (the bracket values are the weight ratios of GO and intercalation polymers).

References

[1] X. Lin, J. R. Varcoe, S. D. Poynton, X. Liang, A. L. Ong, J. Ran, Y. Li, T. Xu, *J. Mater. Chem. A* **2013**, *1(24)*, 7262.

[2] M. S. K. Niazi, M. Hussain, *J. Chem. Eng. Data* **1994**, *39*, 48−49.

[3] M. J. Frisch, G. W. Trucks, H. B. Schlegel, G. E. Scuseria, M. A. Robb, J. R. Cheeseman, G. Scalmani, V. Barone, B. Mennucci, G. A. Petersson, H. Nakatsuji, M. Caricato, X. Li, H. P. Hratchian, A. F. Izmaylov, J. Bloino, G. Zheng, J. L. Sonnenberg, M. Hada, M. Ehara, K. Toyota, R. Fukuda, J. Hasegawa, M. Ishida, T. Nakajima, Y. Honda, O. Kitao, H. Nakai, T. Vreven, J. A. Montgomery, Jr., J. E. Peralta, F. Ogliaro, M. Bearpark, J. J. Heyd, E. Brothers, K. N. Kudin, V. N. Staroverov, T. Keith, R. Kobayashi, J. Normand, K. Raghavachari, A. Rendell, J. C. Burant, S. S. Iyengar, J. Tomasi, M. Cossi, N. Rega, J. M. Millam, M. Klene, J. E. Knox, J. B. Cross, V. Bakken, C. Adamo, J. Jaramillo, R. Gomperts, R. E. Stratmann, O. Yazyev, A. J. Austin, R. Cammi, C. Pomelli, J. W. Ochterski, R. L. Martin, K. Morokuma, V. G. Zakrzewski, G. A. Voth, P. Salvador, J. J. Dannenberg, S. Dapprich, A. D. Daniels, O. Farkas, J. B. Foresman, J. V. Ortiz, J. Cioslowski, and D. J. Fox, Gaussian 09, Revision D.01, Gaussian,

Inc., Wallingford CT, 2013.

[4] J. Liu, N. Wang, L. Yu, A. Karton, W. Li, W. Zhang, F. Guo, L. Hou, Q. Cheng, L. Jiang, D. A. Weitz, Y. Zhao, Nat. Commun. **2017**, *8(1), 2011*.

[5] Y. Han, Z. X, C. Gao, *Adv. Funct. Mater.* **2013**, *23(29), 3693*.

[6] H. Huang, Z. Song, N. Wei, L. Shi, Y. Mao, Y. Ying, L Sun, Z. Xu & X Peng, *Nat. Commun.* **2013**, *4, 2979*.

[7] T. Gao, H. Wu, L. Tao, L. Qu, C. Li, *J. Mater. Chem. A* **2018**, *6(40), 19563.*

[8] L. Huang, J. Chen, T. Gao, M. Zhang, Y. Li, L. Dai, L. Qu, G. Shi, *Adv. Mater.* **2013**, *28(39), 8669*.

[9] K. Goh, W. Jiang, H. E. Karahan, S. Zhai, L. Wei, D. Yu, A. G. Fane, R. Wang, Y. Chen, *Adv. Funct. Mater*. **2015**, *25(47), 7348*.

[10] L. Qiu, X. Zhang, W. Yan, Y. Wang, G. P. Simon, D. Li, *Chem. Commun*. **2011**, *47(20), 5810*.

[11] A. Akbari, P. Sheath, S. T. Martin, D. B. Shinde, M. Shaibani, P. C. Banerjee, R. Tkacz, D. Bhattacharyya, M. Majumder, *Nat. Commun.* **2016**,*7, 10891*.

[12] A. Morelos-Gomez, R. Cruz-Silva, H. Muramatsu, J. Ortiz-Medina, T. Araki, T. Fukuyo, S. Tejima, K. Takeuchi, T. Hayashi, M. Terrones, M. Endo, *Nat. Nanotech*. **2017**, *12(11), 1083*.

[13] H. Huang, Y. Mao, Y. Ying, Y. Liu, L. Sun, X. Peng , *Chem. Commun.* **2013**, *49(53),5963*.